IOSUD - Universitatea Politehnica Timişoara
Şcoala Doctorală de Studii Inginereşti

SOIL - STRUCTURE INTERACTION FOR HYDROTECHNICAL, WATER AND SEWER SYSTEMS AND HYDROAMELIORATIVE STRUCTURES

PHD Thesis – Summary

for obtaining the title of Doctor Engineer

Polytechnic University of Timișoara

in the field of CIVIL ENGINEERING

author ing. Ioan CIORTEA

scientific cooerdinator Prof.univ.dr.ing. Eugen Teodor MAN

May 2019

Chapter 1 The approach of soil - structure interaction for hydraulic enfgineering structures

Hydraulic engineering structures are a part of hydraulic engineering establishments related to hydroelectric energy, water and sewage systems, dams and ripraps. These constructions are of high importance as their damaging or out of service periods my impact crucial aspects of the modern society. From a structural standpoint, they include most structural types of elements ranging from buildings to raft foundations or flood gates. Their annexes include tunnels, channels, canals, pipe supports foundations, water energy dissipators and other.

Vidraru Dam

A few examples of these systems in Romania [12] to be named are Porțile de Fier (1971) dam on Danube river and its upstream and downstream components, the hydroelectric system of Bistrita river, Izvorul Muntelui Dam, with a lake volume of 1230 millions cubic meters, hydropower plant UHE Arges on Arges river and Vidraru dam. With both flood protection and hydroelectric power generation, hydraulic node near Hateg including Gura Apelor dam (highest dam in Romania measuring 168 m in its cross section) and hydroelectric plant CHRMR Raul Mare Retezat.

Water and sewage networks and facilities include special structures necessary for water and

wastewater treatments. These are domestic or municipal and may be placed next to bigger hydraulic engineering structures. The specific types of structures include water intakes, pipe bridges, pumping stations, water tanks, pipe supports foundations and other elements that facilitate the technical processes needed for the water and wastewater treatments. There may also be buildings needed for storage or administrative work.
Soil - structure interaction for these types of structures may vary depending on their size and placement, but its assessment is always necessary for practical and economic design.
Hydroameliorative systems [9] [10] [11] include irrigation and drainage systems, fish ponds or piers for flood protection, along other components used in agriculture and farming [1]. În figures 1-3 distributions of these systems in Romania are presented.

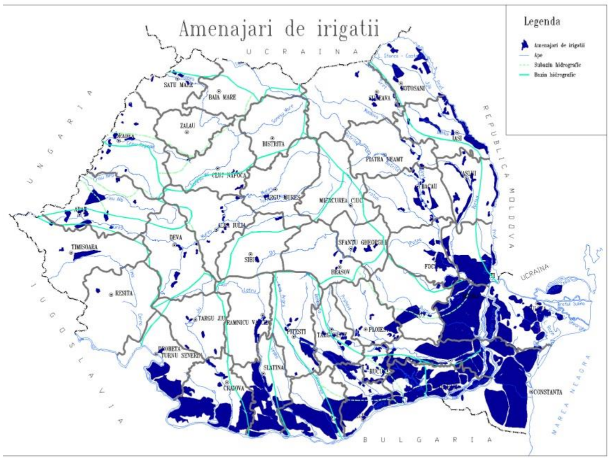

Figure 1. Irrigation distribution in Romania

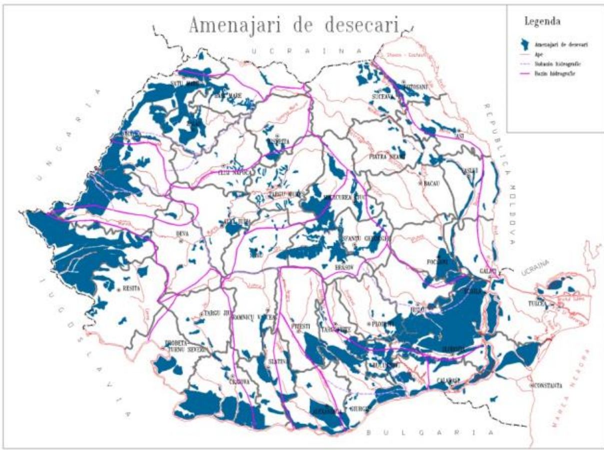

Figure 2. Drainage works distribution in Romania

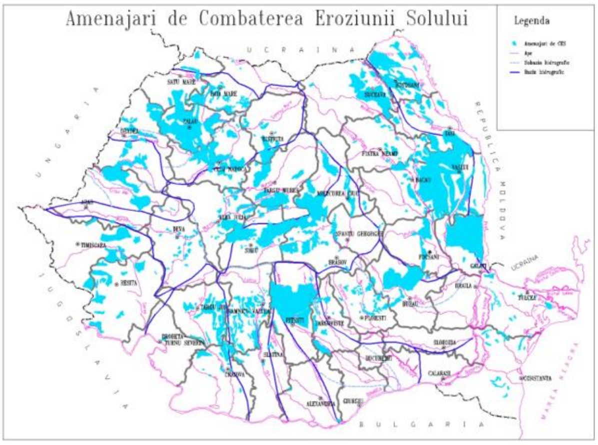

Figure 2. Erosion protection works in Romania

Bad designs and poor maintenance may lead to heavy loses and floods which can have a catastrophic impact on population and the environment. Soil - structure interaction is very important in efficient and sustainable design throughout all of these hydraulic engineering systems.

Chapter 2 Introduction in soil - structure modeling of hydraulic engineering structures

The most common spring type in structural engineering is a nodal link following Hooke's principle [3]:

$$F = kX$$

where k is a characteristic of the linear spring and x the displacement of the spring being pulled by force F. Hooke's law is an accurate approximation for most solid bodies, as long as the forces and deformations are small enough. A graphical representation of Hooke's law may be seen in figure 4.

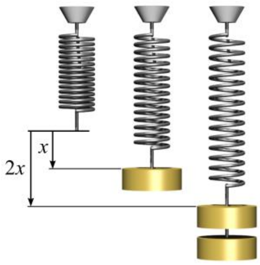

Figure 4. Hooke's Law

Finite element analysis software include linear and nonlinear link elements which can simulate oscillations, hysteretic or plastic behavior. These principles apply to seismic analysis and isolation.

Winkler elastic media was developed by the german professor Emil Winkler as a way to solve the problem of a beam on elastic foundation. The elastic media is made of a linear elastic spring layer of a rigidity proportional to its displacement under load (figure 5).

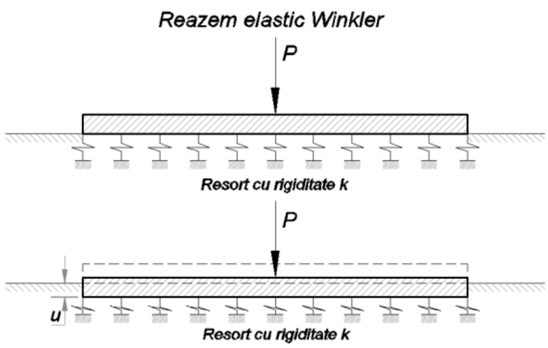

Figure 5. Winkler elastic support

With time many different formulae were presented as to determine the spring stiffness, most of which are based on the compressibility characteristics of the foundation soil.
In figure 6 different values for stiffness k are presented for a C25/30 concrete element (B=1 m, h=0.30 m) resting on a foundation layer with a Poisson's ratio of ν_s=0.35.

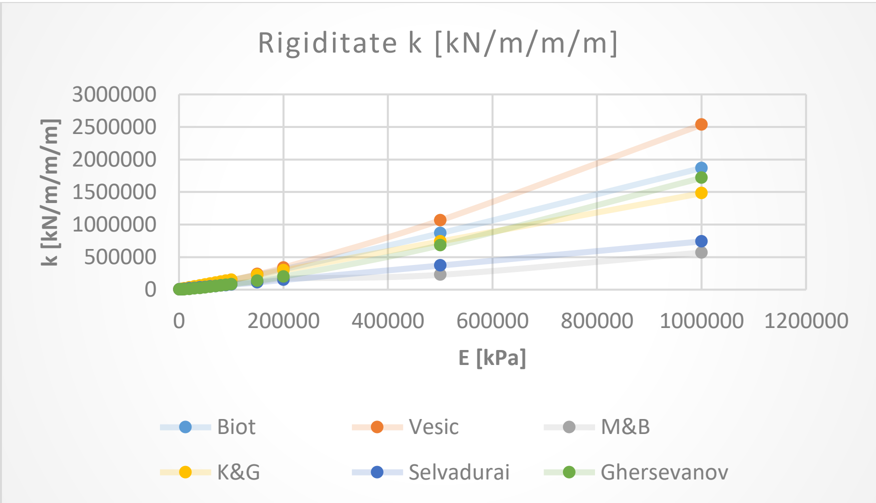

Figure 6. Spring stiffness distribution values

Design recommendations for Winkler type foundations are also found in Annex K of NP112-2014 (romanian norm), modtly for foundation beams under collumns - beams on elastic foundations under concentrated loads. Winkler spring layer stiffness may be written as [4]:

$$p = zk_s$$

where p represents the gravitational load and z the displacement of the loaded node.
One of the biggest disadvantages of Winkler type elastic media is its simplicity and therefore its idealization of the soil - structure interaction. With time experimental tests have shown significant errors in assessing contact pressures and displacements with design calculations and exposing the big limitations of this modeling principle. In 1950 Filonenko-Borodich add an elastic membrane between the spring layer and the structural element with a tension parameter T. Also Hetenyi adds a beam like element (or plate, for spatial modeling) with a bending stiffness while keeping the spring layer. The Pasternak solution (1954) replaces Hetenyi's beam element with a shear element (G parameter) and also keeps the linear spring

layer.

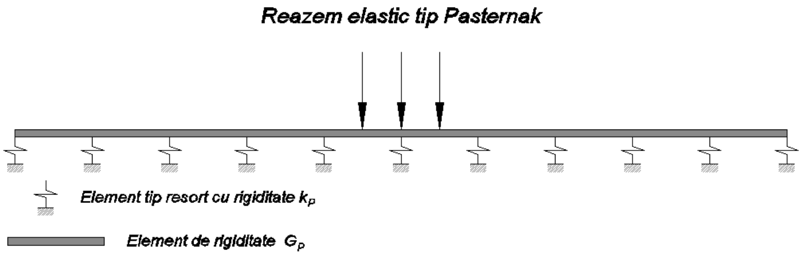

Figure 7. Pasternak Model

The Pasternak's governing equation is as follows:

$$p = k_P w - G_P \nabla^2 w \quad (2.3)$$

where G_P is the shear layer's modulus and w the vertical displacement.

In 1964 Kerr introduces another layer of linear springs (figure 8) between the shear layer and the foundation element.

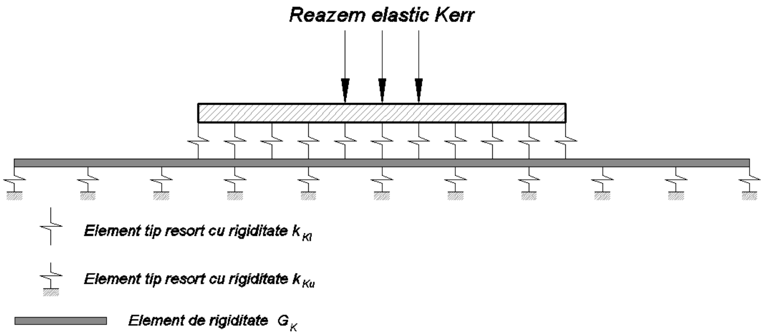

Figure 8. Kerr model

The new equation may be written as follows:

$$(1 + \frac{k_{Ku}}{k_{Kl}})p = \frac{G_P}{k_{Kl}} \nabla^2 p + k_{Ku} w - G_P \nabla^2 w$$

The continuum media is usually modeled using three-dimensional solid elements using finite element analysis [5] either using the theory of elasticity or material curves in a nonlinear analysis. The biggest drawback of this type of modeling is the need for a continuous mesh and maintaining small displacements as per Hooke's law, therefore friction between different elements is very hard to assess.
Solid modeling allows us to perform static and dynamic calculations on complex structures including the foundation layers and view the stress distribution in all the materials contained in the structural model. Figure 9 depicts a small concrete dam [15] from a hydroelectric system. The concrete structure is linked to the foundation media and thus the sliding posibility due to hydrostatic or hydrodynamic pressure is not taken into consideration.

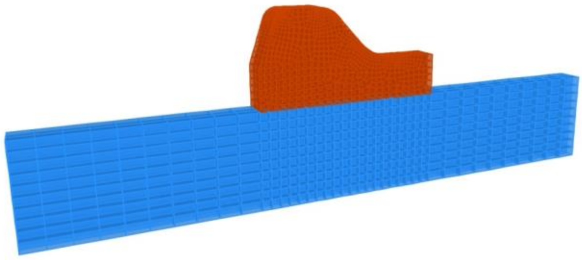

Figure 9. Small concrete dam (solid modeling)

Most of hydraulic engineering structures are subjected to significant horizontal loads which means a high risk of losing stability due to sliding or rollover. To counteract these forces, the friction forces generated between the foundation and the soil are increased due to the weight of the structural element. In this chapter tries to analyze this issue and improve the friction forces that oppose the loads using empiric and experimental scaled tests.
Between the fifth and eighth century experimental studies have led to the formulation of the first two laws of friction by Amontons (1699), followed by the third of Coulomb (1785):
The 1st law of friction: The force of friction is directly proportional to the applied load.
The 2nd law of friction: The force of friction is independent of the apparent area of contact.
The 3rd law of friction: Kinetic friction is independent of the sliding velocity.

Coulomb friction, named after Charles-Augustin de Coulomb is governed by the model:

$$F_f \leq \mu F_n, \text{ where:}$$

F_f – the force of friction exerted by each surface on the other. It is parallel to the surface, in a direction opposite to the net applied force;
μ - the coefficient of friction, which is an empirical property of the contacting materials;
F_n – the normal force exerted by each surface on the other, directed perpendicular (normal) to the surface.

Chapter 3 Reinforced concrete wastewater tank on Winkler elastci support - Case study

The biological wastewater tank [14] is 21 meters long by 24.45 m wide (figure 10). From a technologic standpoint, the tank is divided in two separate tanks (of which is divided into six compartments). The two tanks are separated by a 3 m wide corridor used for maintenance and repairs. The corridor has two floors at +0.10 and +3.10 respectively, while the ground's level is at 97.40 (±0.00) m.a.s.l. The corridor can be accesed through a building next to the tank.

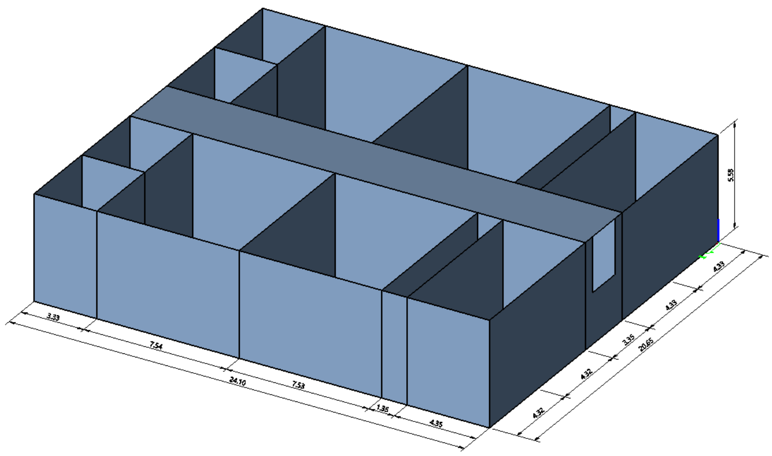

Figure 10. Wastewater biologic tank

The structure was designed in SCIA Engineer with finite element analysis and the reinforcement was calculated as a result. The soil - structure interaction was of a Winkler type elastic media as a layer of springs on the entire surface of the of the raft foundation with the stiffness value of 50000 kN/m^3. For the purpose of analyzing the stress distribution for different spring stiffness 12 values have been taken into consideration.

As a result of the static analysis the stress distribution varies with the increase in spring stiffness, as for an increase of 30% in spring stiffness the internal forces mx and my are lower by about 10-13%. As a result of the structural design it is necessary to determine the stress distribution for different spring stiffness values as an increase of the internal forces in the structural elements may lead to bigger cracks and therefore losing the watertight characteristic.

Chapter 4 Reinforced concrete turbine raft foundation on Winkler elastic media- Case study

The turbines' foundation consists of a reinforced concrete base slab 50 to 80 cm thick. The smaller thickness resulted from the necessity of having multiple channels for maintenance and accidental leaks. All oil or water spills due to malfunction are evacuated through a single channel 27 m long, 30 cm wide and 60 cm deep [15] [13]. The water flow is carried out through 4 circular openings (one for each turbine), each having a 2.35 m diameter, and evacuated to the river by a single reinforced concrete channel. The whole base slab is resting on a compact granular fill (95% Proctor) reaching out to the bed rock, while the channel sits on a C8/10 concrete fill poured directly on the bed rock. Dimensions and overall layout can be seen in fig 11.

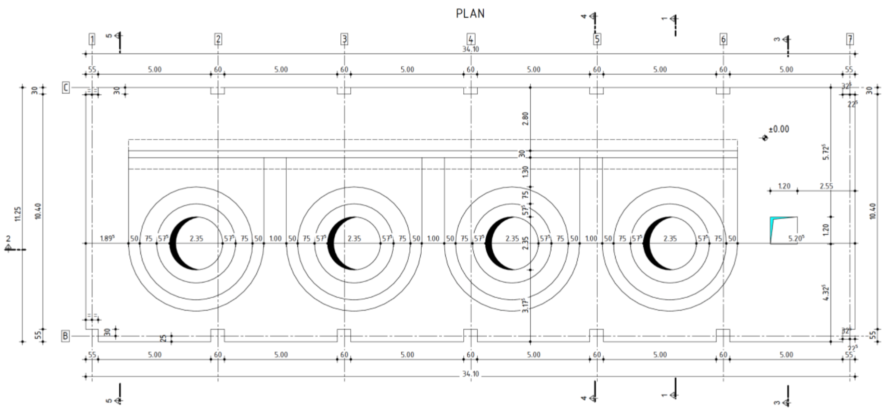

Figure 11. Turbine raft foundation (MHC Săpânța)

Because the elastic media on which each of the elements rests differs (concrete on rock bed for the channel and gravel fill foe the slab), the results obtained for each static model are compared. The elastic media in both cases consists in a Winkler type spring layer. While using Vesic's formula the end result is around 35000 kN/m^3, other values are taken into consideration for the gravel fill, because eventual displacements can lead to higher stress values (table 1). The spring stiffness below the water channel is considered of a constant value of 500000 kN/m^3 (although increasing this value did not lead to higher stress values).

Table 1 - Bending moments

Ks [kN/m/m/m]	M11 (+) [kNm]	M11 (-) [kNm]	M22 (+) [kNm]	M22 (-) [kNm]
15000	166,198	429,138	62,472	441,541
20000	122,222	337,346	53,113	348,238
25000	93,972	276,476	47,078	286,457
30000	81,314	232,747	50,232	242,206
35000	74,48	199,594	52,59	208,863
40000	69,08	173,466	54,405	183,358
45000	64,684	152,266	55,834	167,052
50000	61,024	134,67	56,97	153,455
70000	50,863	88,902	59,789	115,572

Maximum and minimum of M11 and M22 values for different spring stiffness are shown in table 1 for the second static model - the structural system. The bending forces for the simplified model yielded much smaller values due to the fact that the fixed constraints along the channel's walls didn't allow any displacements lead to a very rigid concrete slab. The fact that the maximum values for M11 and M22 were almost ten times smaller means that the slab cannot be computed separately, therefore reinforcement calculation is based on the second (and the more complex) model.

Chapter 5 Base slab on Kerr and Pasternak - Kerr elastic media - Case study

This chapter includes a case study of a static analysis for a concrete slab on elastic foundation using finite element analysis software SAP 2000 [7]. The goal is to analyze the behavior of a concrete element for multiple elastic media - Kerr, Pasternak - Kerr and Winkler - in comparison to the solid modeling. The accuracy of the results will pe assessed for practical use in structural design scenarios. Kerr and Pasternak - Kerr elastic supports are an attractive multi parameter solutions for a wider range of structures [34] [8].

In this case study a base slab of 5 m long by 4 m wide and a height of 25 cm is placed on Kerr, Pasternak - Kerr [6] and Winkler type elastic supports and compared to a homogeneous media comprised of solid elements.

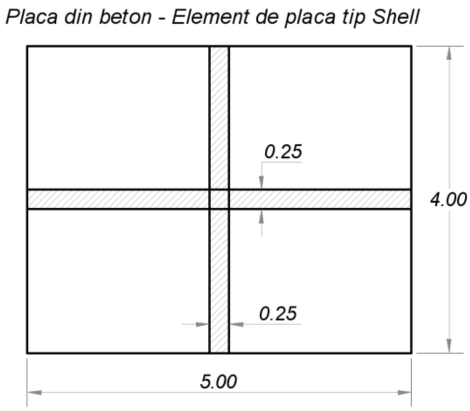

Figure 12. Base concrete slab

There are five load cases considered:

- Load case 1 - Uniform distributed load on the slab's edges, 20 cm wide, simulating a concrete wall 3 m high;
- Load case 2 - Point load from a column in the center of the slab on a 30 x 40 cm area;
- Load case 3 - Uniform surface load on half of the slab's surface;
- Load case 4 - Uniform surface load distributed on a quarter of the slab's surface;
- Load case 5 - Uniform surface load distributed on the whole plate surface.

The Kerr type elastic support [6] is shown in figure 13.

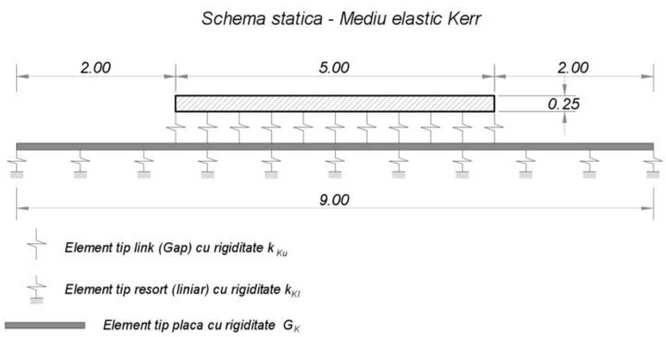

Figure 13. Kerr Model

The Pasternak - Kerr type elastic support is obtained by reducing the previous model to two parameters - k_P and G_P - as shown in figure 14.

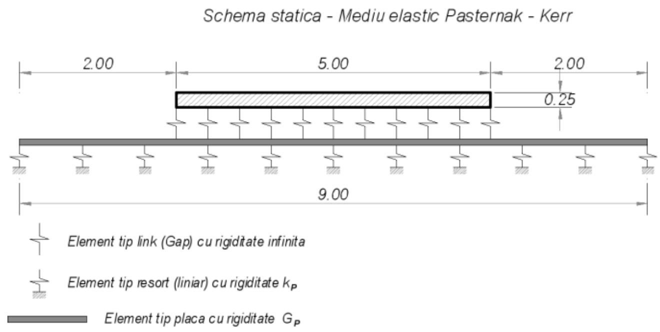

Figure 14. Model Pasternak - Kerr

The solid elements divided into mesh cubes is shown in figure 15

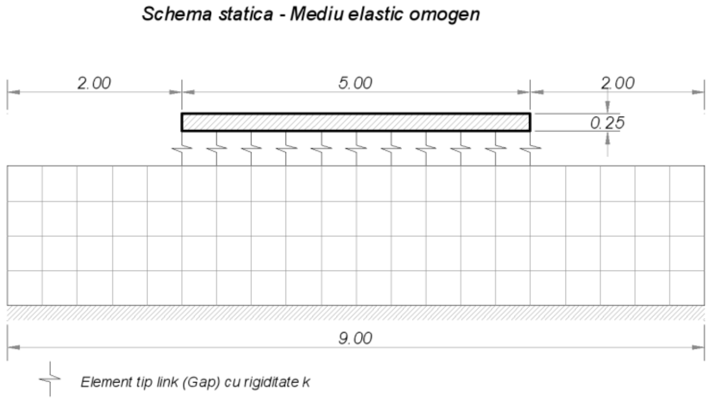

Figure 15. Solid modeling

The Winkler type elastic support is modeled as a single layer of linear springs (figure 16) with the proportional stiffness between the applied load and the displacement of the nodes.

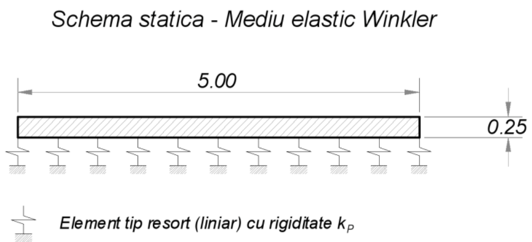

Figure 16. Winkler elastic support

Because of the multiple parameters (load cases, Young's modulus, elastic supports) the result comparison is presented as deviations in regard to the solid modeling. The deviations are calculated as an error:

$$\frac{|b_{med}-a_{med}|}{a_{med}} \cdot 100\ \% \ = \ E_{med}[\%], \text{ unde:}$$

a_{med} - medium displacement of nodes (x sau y) calculated as an average of displacements for the solid elastic media for each elastic modulus;
b_{med} - medium displacement of nodes (x sau y) calculated as an average of displacements for

the Kerr(H), Pasternak - Kerr and Winkler respectively elastic media for each elastic modulus valoarea medie a deplasării nodale pe direcția principală (x sau y) a plăcii, obținută prin media E_{med} - deviation of each elastic support media displacements in regard to the solid modeling în percents.

A smaller value of the deviation (E_{med}) means a more precise exact solution in regard to the solid model. The solid model is considered the most accurate due to the direct integration of the material parameters (E, ν). The procentual values of the deviations are relative to the solid analysis which is considered the correct value at 100%.

Chapter 6 Case study for bending moments and displacements for a finite beam on elastic foundations

Contact problems refer to the soil - structure interaction and the way the stresses in the element are transmitted to the foundation layer. In hydraulic engineering and most types of foundations we encounter two cases: a rigid foundation placed on softer elastic bed (figure 17 a) and a large deformable structural element placed on elastic media (figure 17 b). The first case includes classic concrete foundations as well as massive rigid elements such as dams, pipe anchor foundations and rigid concrete retaining walls, while in the second category we see raft foundations, storage tanks, base slabs and platforms.

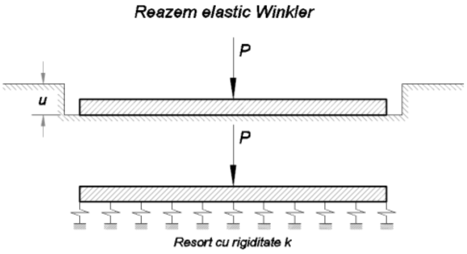

a

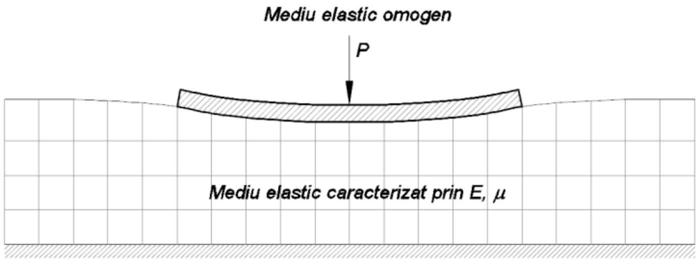

b

Figure 18. Rigid body on Winkler foundation (a) and flexible body on solid elements (b)

In hydraulic engineering bending causes cracks in concrete elements and the watertight characteristic is lost. These types of structures are also quite large which makes modeling complicated elastic supports a tedious process. In this chapter the author aimed to correct the spring stiffness for a Winkler type elastic support considering a concrete beam on an elastic foundation. The goal is to determine a more precise way of calculating the bending moments of this element, using finite element analysis based SAP 2000 software, and comparing to a solid modeling of the foundation layer, which is considered the more accurate structural model (figure 18). The beam sections, the materials and the loads will be the same for both models (figure 19).

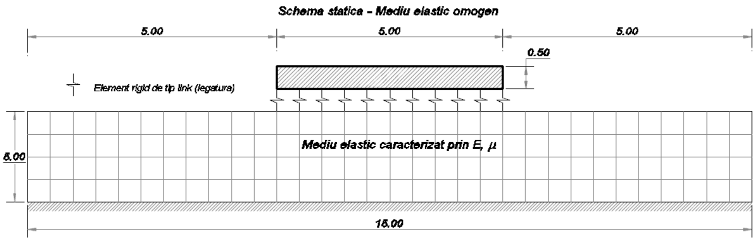

Figure 18. Beam on continuous elastic media (solid)

Figure 19. Beam on Winkler type elastic support

The static analyses was run on two distinct load cases, a single concentrated load (P=250 kN) at the middle point of the beam and a uniform distributed load q=50 kN/m.
On the Winkler model the static analysis yielded smaller values for the bending moment under the uniform distributed load. This can be counter balanced by modifying the spring stiffness on the entire layer (lower values) or changing the values of some of the node springs' stiffness. Both of these principles will be studied in this chapter.
For a soil's young modulus of E=210000 kPa, uniform distributed load of q=50 kN/m and a spring layer stiffness of k=27204 kN/m (Winkler type elastic support, Biot's formula) we can calculate the displacement of each of the nodes (figure 20) adn then the load P=uk corresponding to each of the beam's nodes.

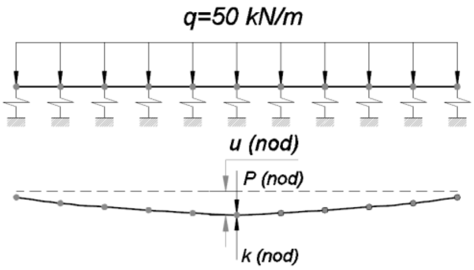

Figure 20. Static model for calculating P load

With the determined value for load P corresponding to each node, by dividing it to the displacement of the node in solid modeling elastic support, we get a new spring stiffness ”k calculat”. The difference in spring stiffness is around 12%, meaning that for a more accurate representation we need to decrease the theoretic spring stiffness by around 12% (initial value as per Biot's formula, k_c=23940 kN/m). For the initial spring stiffness of k_c=23940 kN/m we have a bending moment of M=6.84 kNm, while for the solid modeling structural model the bending moment has a value of 11 kNm.

For smaller stiffness values of the spring layer (k_c=8379 kN/m) the bending moment increases to 11.01 kNm (as the solid modeling reference), but displacements are almost 3 times larger, therefore this correction cannot be used for accurate design practices. The static analysis data has indicated that for smaller spring stiffness values (and smaller soil Young's modulus) for larger displacements we get a more pronounced bending in the structural element.
For the concrete beam in presented earlier we have determined an optimum of 1.5 increase in k as calculated with Biot's formula. This leads to a bending moment of M=10.76 kNm or M=11.13 kNm for 1.5k. These results are valid for a mesh of 11 linear elements (L/10) and 11 nodes, each linear element of 0.50 m length. For a more refined mesh (L/20 and L/40) we need to use 2.5k and 4.5k respectively or distributing the 1.5k springs to a larger area of around 1/10th of the beam on each side.

Capitolul 7 Stabilitatea la alunecare a fundațiilor

To increase sliding stability sometimes a sill like element is added to the base of the foundation to increase the friction resistant force. Another objective is to measure the kinetic friction forces and the kinetic coefficient of friction for concrete foundations placed on sandy and gravely soil [16] [18]. The kinetic coefficient of friction can have significant values and therefore may increase the bearing capacity of the horizontal loaded foundation.
The element needs to be bigger as the soil's shear strength decreases. The smaller the element, the bigger the shear pressure which overcomes the soil's yield strength and the foundation begins to slide. The principle is shown. in figure 21.

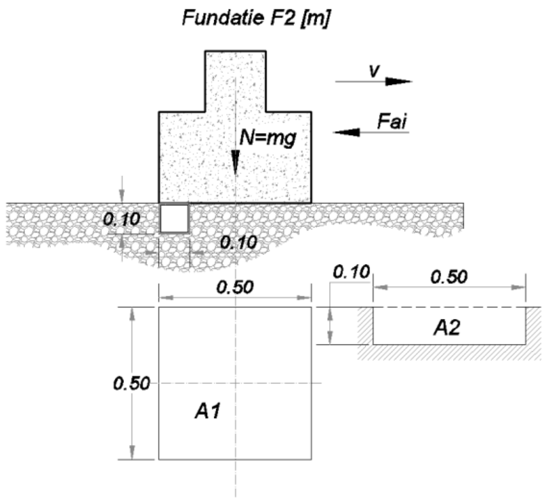

Figure 21. Prismatic rugosity on a concrete foundation

Figure 21 shows a concrete foundation with a 0.50x0.50 m base and a steel sill like element with a 100x100 mm rectangular cross section, while A_1 and A_2 are the contact surfaces between the foundation and the foundation layer. Considering the plowing effect given by the steel element (as increased roughness) we may write:

$$\mu_b = \frac{F_{ai}}{F_{ni}} = \frac{A_2 \cdot \tau}{A_1 \cdot \sigma_c}$$

unde A_1 și A_2 reprezintă amprenta fundației pe terenul de fundare respectiv suprafața de material brăzdat, iar τ efortul de forfecare admisibil al terenului de fundare.

We will attempt to calculate the friction forces with and without increasing the foundation's base roughness, followed by an experimental study by which we will measure the coefficients of friction for both static and kinetic friction.

The test stand was constructed as two box shaped areas, one for each soil type. The foundations were laid on each of the soil surface and pushed horizontally, while horizontal and vertical displacements were measured along with the pushing force. For this particular study four foundation types and two types of soil were analyzed (figure 22).

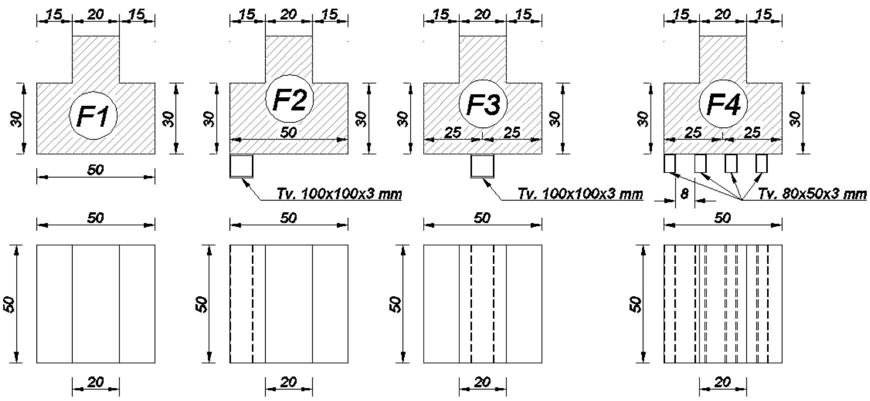

Figura 22. Concrete scaled foundations

The experimental tests are conducted on four concrete foundations of 1:2 scale (figure 22), while the base rugosity was added as a rectangular steel profile. The friction forces were measured for each of the two soil types, sandy soil and a granular recycled material similar to gravel.

The maximum values of the pushing forces and displacement are as follows:

Teren 1
F1 - 2,28 kN - 12,62 mm
F2 - 1,81 kN - 34,02 mm
F3 - 1,89 kN - 21,82 mm
F4 - 1,40 kN - 11,12 mm

Teren 2
F1 - 1,77 kN - 8,06 mm
F2 - 3,41 kN - 8,44 mm
F3 - 3,53 kN - 6,06 mm
F4 - 2,40 kN - 7,57 mm

The principle above can be used to increase the friction forces that oppose sliding in sill like elements and small dams, as well as different types of foundations for industrial equipment. The goal of the experimental tests was also to assess the kinetic friction forces that occur after the foundations start to slide and the impact of the added steel rugosity to the sliding motion.
The added resistant force should be considered as a reserve capacity for accidental loads, but with careful research over a wide variety of soils and foundation models it may serve design engineers as a way of design optimization for certain foundation types. The author recommends further research by applying the principles stated above to numerous soils and load curves for better understanding of the kinetic resistant friction forces.

Chapter 8 Conclusions and author's contributions

Because of the complicated nature of the hydraulic engineering structures, the soil - structure interaction in extremely important in structural design due to the possibility of degrading over time and lose of sealing. Also the need of these kind of structures in densely populated areas increases the risk of accidents.
This paper contains a synthesis of procedures for practical design of such structures and the modeling of their foundations using elastic media for modeling the foundation layers. The emphasis is put on stresses and displacements and improving accuracy of said values for efficient and sustainable designs. The new elastic media modeling solutions as Kerr and Pasternak - Kerr are also presented and tested for practical uses in structural design for base slabs, raft foundations or industrial equipment foundations.
The sliding stability, a known problem for foundations under large horizontal loads is also addressed in this thesis with an alternative to increasing the friction forces that oppose the loads.
The goal of this paper is improving structural design accuracy and eventually adding algorithms and recommendations to the specific design norms and laws for more efficient and sustainable structures.

Author's contribution can be summarized as follows:

1) Compiling a large list of complex references relevant to structural design and design practices all over the world and soil - structure interaction;

2) Providing a list of formulae for calculating Winkler type media spring layer stiffness while

adding the romanian specific stipulations;

3) Applying Winkler type elastic support for two structures (biological wastewater tank and turbine raft foundation) for studying the stress distribution for multiple soil types;

4) Applying Kert and Pasternak - Kerr type elastic supports for hydraulic engineering specific structures

5) Using Kert and Pasternak - Kerr type elastic supports for practical use and comparing the results with Winkler type media and solid modeling. This can be seen throughout chapter 5 which includes detailed finite element analysis;

6) Adding corrections to Winkler type elastic supports for practical use. The calculation was conducted on an elastic supported concrete beam;

7) Compiling a list of procedures for calculating friction forces for pipe support foundations;

8) Use of plowing friction theory for concrete foundations sliding stability applied to pipe supports concrete foundations;

9) Presenting a proposed algorithm for added rugosity on foundations' bases using plowing friction theory;

10) Testing the plowing friction theory on scaled concrete foundations in an experimental stand both in static and kinetic situations;

11) Measuring the friction forces and coefficients of friction after foundation sliding is encountered on scaled concrete foundations.

Chapter 9 References

[1] Măgdălina I., Mărăcineanu F., Cismaru C., Man E.T., Exploatarea lucrărilor de îmbunătăţiri funciare, Editura Didactică şi Pedagogică, Bucuresti, 1983
[2] http://www.anif.ro/cnrid/contributii/art-drnicolescu/
[3] Legea lui Hooke - Wikipedia (https://en.wikipedia.org/wiki/Hooke%27s_law Hooke wikipedia)
[4] NP112-2014 – Normativ privind proiectarea fundațiilor de suprafață
[5] Mecanica solidelor - Wikipedia (https://en.wikipedia.org/wiki/Solid_mechanics)
4]15] S.C. ISPE S.A., Documentație tehnică ”Captare Valea Trei Săpânți”, contract
[6] Asrat Worku, Development of a calibrated Pasternak foundation model for practical use, International Journal of, Geotechnical Engineering vol. 8, No. 1, 2014
[7] CSI Analysis Reference Manual For SAP2000®, ETABS®, SAFE® and CSiBridge™, ISO# GEN062708M1 Rev.5 Berkeley, California, USA, may 2011
Hideaki Tanahashi, Formulas for an infinitely long Bernoulli - Euler beam on the Pasternak model, SOILS AND FOUNDTIONS Vol. 44, No. 5, 109-118, Oct. 2004, Japanese Geotechnical Society
[8] AD C. Pronk and Marion E. van den Bol, Winkler – Pasternak – Kerr Foundations – Notes on Boundary Conditions, BCRA`98 conference in Trondheim
[9] Man T.E., Exploatarea sistemelor de îmbunătăţiri funciare, Litografia Universităţii Tehnice Timişoara, 1983

[10] Man T.E., Sabău N.C., Cîmpan G., Bodog M., Hidroamelioraţii, Editura Aprilia Print, Timişoara, 2007 (Red. 2008)
[11] Man,T.E.,Drenaje vol.I si II, Editura Orizonturi universitare, 2014, Timisoara, ISBN 978-973-638-565-0
[12] Radu Prișcu, CONSTRUCȚII HIDROTEHNICE VOL. I, Editura Didactică și Pedagogică București
[13] I. Ciortea, A. Feier, M. Muntean and E. Man, "CASE STUDY OF TURBINE FOUNDATION. METHODS TO REDUCE CONCRETE VOLUME", **SGEM International GeoConferences**, **28 June - 7 July, 2016** at Albena Resort, Bulgaria
[14] S.C. ISPE S.A. Sucursala Timișoara, Documentație tehnică "Lot 2. Realizare stație de epurare nouă în Recaş"
[15] S.C. ISPE S.A., Sucursala Timișoara, Documentație tehnică "Poz. 2.2. Clădire microhidrocentrală Săpânța", contract "Amenajare potențial hidroenergetic râu Săpânța
[16] WIKIPEDIA.ORG – Surface Roughness
[17] SC ISPE SA, Mărirea stabilității depozitului de zgură și cenușă mal drept Jiu cota 122 mdMB – Compartiment II SE Ișalnița – Proiect tehnic și detalii de execuție – Supraînălțare deposit zgură și cenușă mal drept jiu cota 122 mdMB
[18] Departamentul de Organe de Maşini şi Tribologie, Secțiunea Didactic - Link